ACS APPLIED MATERIALS & INTERFACES

Research Article

www.acsami.org

Stretchable and Micropatterned Membrane for Osteogenic Differentation of Stem Cells

Xuetao Shi,*[,†] Lei Li,[§] Serge Ostrovidov,[†] Yiwei Shu,[‡] Ali Khademhosseini,[†,∥,⊥,⊗] and Hongkai Wu*[,†,‡]

[†]WPI-Advanced Institute for Materials Research, Tohoku University, Sendai 980-8578, Japan

[‡]Department of Chemistry, Hong Kong University of Science & Technology, Hong Kong, China

[§]Beijing Key Laboratory of Cryo-Biomedical Engineering and Key Laboratory of Cryogenics, Technical Institute of Physics and Chemistry, Chinese Academy of Sciences, Beijing 100190, China

[∥]Center for Biomedical Engineering, Department of Medicine, Brigham and Women's Hospital, Harvard Medical School; Harvard-MIT Division of Health Sciences and Technology, Massachusetts Institute of Technology; Wyss Institute for Biologically Inspired Engineering, Harvard University, Boston, Massachusetts 02115, United States

[⊥]Department of Maxillofacial Biomedical Engineering and Institute of Oral Biology, School of Dentistry, Kyung Hee University, Seoul 130-701, Republic of Korea

[⊗]Department of Physics, King Abdulaziz University, Jeddah 22254, Saudi Arabia

Supporting Information

ABSTRACT: Stem cells have emerged as potentially useful cells for regenerative medicine applications. To fully harness this potential, it is important to develop in vitro cell culture platforms with spatially regulated mechanical, chemical, and biological cues to induce the differentiation of stem cells. In this study, a cell culture platform was constructed that used polydopamine (PDA)-coated parafilm. The modified parafilm supports cell attachment and proliferation. In addition, because of the superb plasticity and ductility of the parafilm, it can be easily micropatterned to regulate the spatial arrangements of cells, and can exert different mechanical tensions. Specifically, we constructed a PDA-coated parafilm with grooved micropatterns to induce the osteogenic differentiation of stem cells. Adipose-derived mesenchymal stem cells that were cultured on the PDA-coated parafilm exhibited significantly higher osteogenic commitment in response to mechanical and spatial cues compared to the ones without stretch. Our findings may open new opportunities for inducing osteogenesis of stem cells in vitro using the platform that combines mechanical and spatial cues.

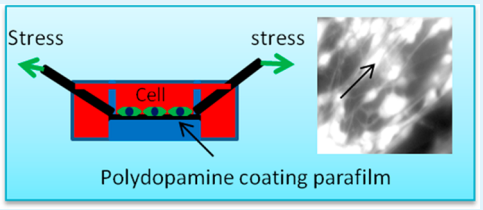

KEYWORDS: *parafilm, polydopamine, stretchable materials, micropattern, mechanical tension, cell behavior*

1. INTRODUCTION

Stem cells possess great potential in enabling regenerative medicine for a range of ailments.[1−3] Nevertheless, before stem cells can be clinically transplanted, an understanding of the mechanisms underlying stem cell behavior in injured tissue is necessary.[4] A number of studies have confirmed that transplanted undifferentiated stem cells may have serious side effects.[5,6] For example, transplanting stem cells directly into injured tissue not only fails to trigger specialized commitment but may induce tumorigenesis.[7] Thus, generating an in vitro cell culture platform to differentiate stem cells prior to clinical use is necessary.

The periosteum is a fibrous membrane which covers the surface of bones.[8] The inner layer of the periosteum (also known as cambium/osteogenic layer) has a microarchitecture made of longitudinally assembled cells and collagen fibers. This layer is important in the growth, remodeling, and fracture repair of bone.[9−15] Stem cells residing in this layer are highly mechanosensitive and alter the production of numerous signaling molecules when triggered by a mechanical stimulus.[16−25] To mimic the periosteum and differentiate stem cells into osteogenic phenotypes, it is necessary to construct a platform that enables the regulation of cell morphologies and behavior (including proliferation and differentiation) using a combination of mechanical and topographical cues.[25−30]

To construct a platform that combines spatial and mechanical cues for inducing the differentiation of stem cells in vitro, the substrate for cell culture should possess excellent stretchability and processability. Conventional cell culture materials often do not fulfill these requirements. In this study, we used parafilm as a model material to construct a cell culture platform that combines topographical and mechanical cues to induce osteogenic differentiation of stem cells. Parafilm is a flexible thermoplastic film that is commonly used for sealing and protecting various reagent-containing vessels because of its superb waterproofing, cohesion, and ductility properties. Parafilm-based microfluidic devices have been developed for low-cost diagnostic applications.[31] Compared with conventional

Received: October 22, 2013
Accepted: June 30, 2014
Published: June 30, 2014

 © 2014 American Chemical Society

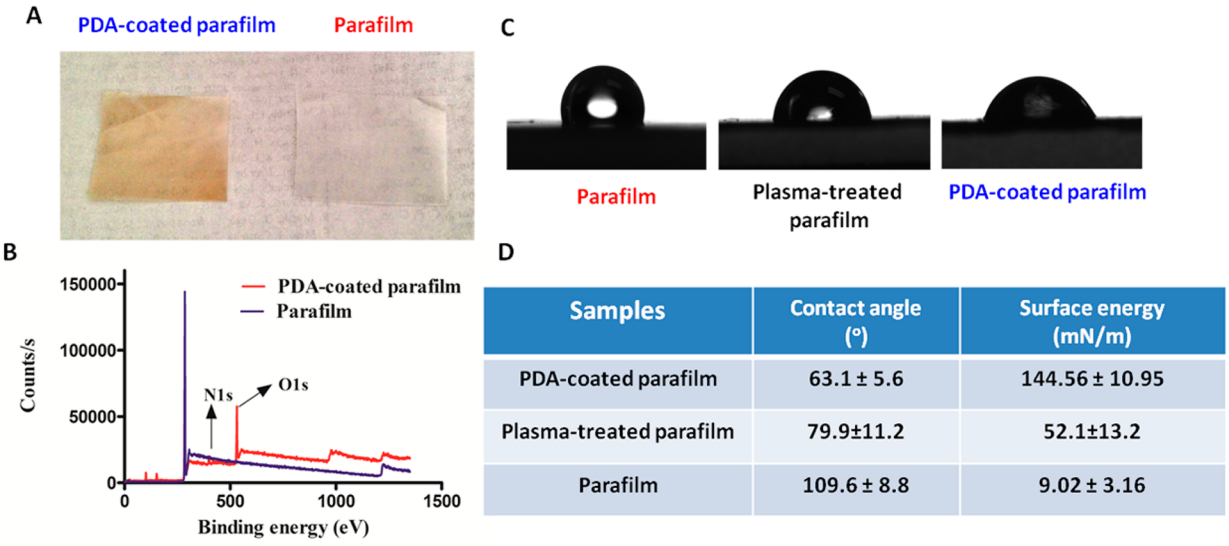

Samples	Contact angle (°)	Surface energy (mN/m)
PDA-coated parafilm	63.1 ± 5.6	144.56 ± 10.95
Plasma-treated parafilm	79.9±11.2	52.1±13.2
Parafilm	109.6 ± 8.8	9.02 ± 3.16

Figure 1. Surface property of the PDA-coated parafilm and pristine parafilm. (A) Images of the PDA-coated parafilm and pristine parafilm. (B) XPS survey scan spectra of the surfaces of the PDA-coated parafilm and pristine parafilm. (C and D) Wettability and surface energy of the PDA-coated parafilm and pristine parafilm.

stretchable matrices, parafilm displays a higher stretchability.[31] Moreover, it has a low cytotoxicity and is readily available in most chemical, engineering, and biological laboratories. Importantly, to mimic the microenvironment of periosteum, it is not necessary to have an elastic deformation. Here, due to the significant elongation of natural periosteum, we wanted a material that could elongate more than two folds than its original length after stretching. As a proof-of-concept material that possesses this property, we chose parafilm as the substrate for simulating periosteum in vitro. However, the high surface hydrophobicity of parafilm (similar to that of polydimethylsiloxane (PDMS)) prevents cells from attaching to its surface. To surmount this obstacle, a chemical/physical surface modification is required.

The biological applications of polymer coatings have long been studied. For example, to promote cell adhesion, polylysine is commonly utilized as a coating in PDMS-based microfluidic devices and to coat cell culture dishes.[32,33] However, polylysine coating is not stable over long periods. An alternative strategy for generating a stable polymer coating on various hydrophobic surfaces that has received recent attention is the use of polydopamine (PDA).[34−36] PDA is a synthetic polymer that is derived from dopamine, a small molecule that is an important neurotransmitter.[37] A unique feature of PDA is its ability to deposit on various hydrophilic or hydrophobic surfaces via self-polymerization by the oxidation of dopamine in a weak alkaline buffer solution.[38] The biocompatibility of the PDA coating on various materials has been evaluated, and the results indicate that the PDA coating can facilitate the adhesion of different cell types, including fibroblasts, endothelial cells, osteoblasts, and neural cells.[39,40] Moreover, PDA coatings can also be useful to immobilize proteins, enzymes, and growth factors via covalent coupling without altering their bioactivities.[41,42]

In this study, we used surface modified parafilm to regulate cell behavior (such as cell alignment and cell differentiation). Parafilm was coated with PDA to induce cell adhesion. In addition, various motifs were generated on the modified parafilm by using soft lithography. To evaluate stem cell differentiation on the platform, we analyzed the osteogenic differentiation of adipose-derived mesenchymal stem cells (ADMSCs). ADMSCs can be easily derived from adipose tissue with minimal site morbidity, and have excellent self-renewal and proliferation properties. We cultured ADMSCs onto the platform with grooved micropatterns, and different mechanical tensions were exerted onto the modified parafilm to simulate the microstructure and mechanical stresses of the natural periosteum. We hypothesized that the platform may be used to modulate the osteogenic commitment of stem cells by the combination of topographical, mechanical, and biological cues.

Although there are numerous publications on the topics of stretch or micropatterns induced or promoted the osteogenesis of stem cells or osteoblasts, the combination of mechanical and topographic cues by mimicking the microenvironments of stem cells on the periosteum has not been fully investigated.[42−44] In this study, an in vitro platform was constructed for inducing osteogenesis of stem cells by simulating the microenvironment of periosteum. Our findings may open new opportunities for inducing osteogenesis of stem cells for the application of regenerative medicine and for the study of physiological differentiation of periosteum during osteogenesis in vitro.

2. EXPERIMENTAL SECTION

2.1. Preparation of Micropatterned PDA-Coated Parafilm. Prepolymer (TSE3032, Momentive, Japan) was cured to produce microgrooved PDMS stamps (with groove spacings of 30, 50, and 100 μm) with different micropatterns on a master fabricated by conventional photolithography technique using SU-8 photoresist. Parafilm (Pechiney Plastic Packaging Company, USA) was covered by a flat poly(methyl methacrylate) (PMMA) chip and the PDMS stamp, and then was heated using a hot compressor (Taiming, Inc., USA) for 3 s at 60 °C. The sandwich assembly was cooled down to ambient temperature, and then removed the PMMA chip and PDMS stamp. The obtained micropatterned parafilm was treated with oxygen plasma for 5 min. Subsequently, the resulting micropatterned parafilm was dipped into a 2 mg/mL dopamine (Sigma-Aldrich, USA) Tris buffer (10 mM) solution at pH 8.5. The polydopamine coating was generated by the autopolymerization of dopamine. After 8 h, an observed polydopamine coating was obtained on the micropatterned parafilm. The XPS spectra were conducted on a Kratos Photoelectron Spectrometer (Kanagawa, Japan).

2.2. Wettability. The contact angles of the flat PDA-coated parafilm and flat pristine parafilm were measured on a contact angle meter (Kyowa Kaimenkagaku Co., Saitama, Japan). The surface free energy of PDA-coated parafilm was calculated using the following equations:

$$(1 + \cos\theta_w)\gamma_w = 4(\gamma_w^d\gamma_s^d/(\gamma_w^d + \gamma_s^d) + \gamma_w^p\gamma_s^p/(\gamma_w^p + \gamma_s^p))$$

and

$$(1 + \cos\theta_g)\gamma_g = 4(\gamma_g^d\gamma_s^d/(\gamma_g^d + \gamma_s^d) + \gamma_g^p\gamma sp/(\gamma_g^p + \gamma_s^p))$$

where γ^d and γ^p are the dispersive and polar component and θ_p and θ_w are the contact angles to glycerin and water, respectively.

2.3. Protein Immobilization. One milliliter of 50 μg/mL fibronectin (or rhodamine labeled-fibronectin solution) (in deionized water solution), or 100 μg/mL bovine serum albumin (BSA) (or fluorescein isothiocyanate (FITC) labeled-BSA solution) (in deionized water solution) was added to the surfaces of the flat pristine parafilm and flat PDA-coated parafilms (1 × 1 cm), and then incubated in room temperature in an incubator. After 5 h, the films were carefully washed with deionized water solution, and then placed into 1% sodium dodecyl sulfate to remove the non-covalent proteins on their surface. A protein assay kit (QuantiPro bicinchoninic acid protein assay kit, Sigma-Aldrich, USA) was used to test the total protein absorbed on the surfaces of films.[45]

2.4. Cell Seeding and Viability. The PDA-coated parafilm pieces were placed under the UV light of a clean bench for 30 min. Samples (flat pristine parafilm, flat parafilm treated with plasma, flat PDA-coated parafilm, micropatterned PDA-coated parafilm with groove spacings of 30, 50, and 100 μm; all 2 × 2 cm) were respectively loaded with 100 μL of ADMSC (DS Pharm Biomedical, Japan) suspension (5 × 10^5 cells/mL) and incubated in an incubator for 3 h and then a cell culture medium (Dulbecco's modified Eagle's medium (DMEM)/F12 supplemented, 1% streptomycin/penicillin (Invitrogen, USA), 10% (v/v) fetal bovine serum (FBS, Invitrogen, USA), and HEPES (to regulate the pH value of medium to 7.4, Sigma-Aldrich, USA)) were used for cell culture. The cell viability was determined using Live/Dead cell viability/cytotoxicity kit (Invitrogen) according to the manufacture's instruction. Cell Counting Kit-8 (Sigma-Aldrich, USA) was used for the determination of viable cell number on the films.

2.5. Quantification of Cell Alignment. To quantify the degree of cellular alignment, cells on the micropatterned PDA-coated parafilm with groove spacings of 30, 50, and 100 μm were stained with 4',6-diamidino-2-phenylindole (DAPI) (for the cell nuclei) and rhodamine-phalloidin (Invitrogen; for F-actin), respectively. The angles of cell and nuclei alignment were measured by the method described in the references.[46−48]

2.6. Determination of the Cell Numbers on PDA-Coated Parafilms. One hundred microliters of ADMSC suspension (5 × 10^5 cells/mL) was added onto PDA-coated parafilm (2 × 2 cm) with groove spacing of 50 μm. After 1 day of culture, a low force (2 N) or a high force (2.5 N) was utilized to stretch PDA-coated parafilm strips. The force was maintained for 5 days. Cell Counting Kit-8 (Sigma-Aldrich, USA) was used for the determination of viable cell number on the films.

2.7. Fabrication of a Device Based on PDA-Coated Parafilm to Induce Cell Strain. To induce the elongation of a cell cultured on the micropatterned PDA-coated parafilm, we designed a PDMS device, which is shown schematically in Figure 6A. A small PDMS chamber was placed in a cell culture dish, and rectangular holes were cut through the right and left walls of the PDMS chamber, respectively. A strip of micropatterned PDA-coated parafilm was inserted through the two holes, and forces were exerted at the ends of the parafilm strip to stretch the parafilm, creating strains on the ADMSCs cultured on the parafilm. The center of the parafilm strip that has grooved micropatterns (the groove is 50 μm and the micropatterned area is 6 × 6 mm) in the small PDMS pools in the as-prepared devices were loaded with 200 μL of ADMSC suspension (1 × 10^4 cells/mL), and a low force (2 N) and high force (2.5 N) were utilized to stretch the strips after 1 day of culture in the cell culture medium. The tensile

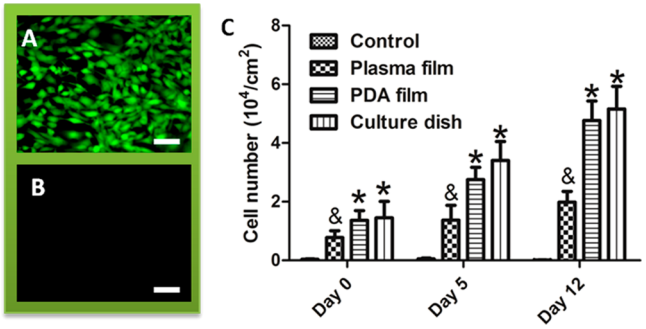

Figure 2. Cell viability and proliferation on PDA-coated parafilm. (A and B) Fluorescent images of cells on the PDA-coated parafilm and the pristine parafilm stained by the live/dead kit. (C) Cell proliferation on the PDA-coated parafilm, plasma treated parafilm, pristine parafilm, and culture dish (scale bar: 100 μm).

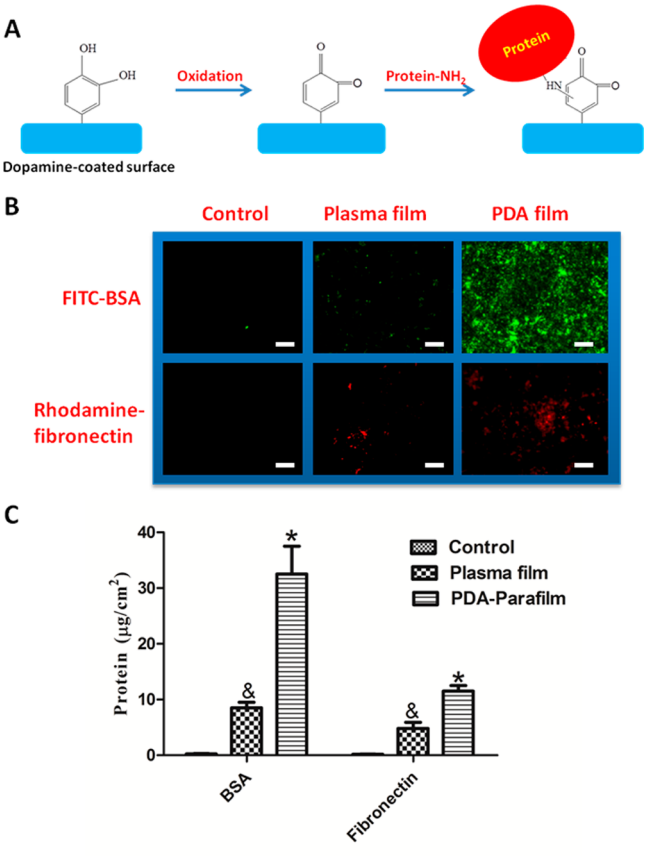

Figure 3. Protein immobilization on the PDA-coated parafilm. (A) Schematic of protein immobilization on the PDA-coated parafilm. (B) Fluorescent images of the fluorescein isothiocyanate labeled-bovine serum albumin (FITC-BSA) and rhodamine-fibronectin immobilized on the parafilm (control), oxygen-plasma-treated parafilm (plasma parafilm), and PDA-coated parafilm (PDA parafilm), respectively. (B) Fluorescent images of immobilized on the parafilm (control), oxygen-plasma-treated parafilm (plasma parafilm), and PDA-coated parafilm (PDA parafilm), respectively. (C) Quantification of protein immobilized on the pristine parafilm (control), oxygen-plasma-treated parafilm (plasma film), and PDA-coated parafilm (PDA film). The * and & symbols indicate statistical significance when compared with cells cultured on the oxygen-plasma-treated parafilm and parafilm, respectively (scale bars: 100 μm).

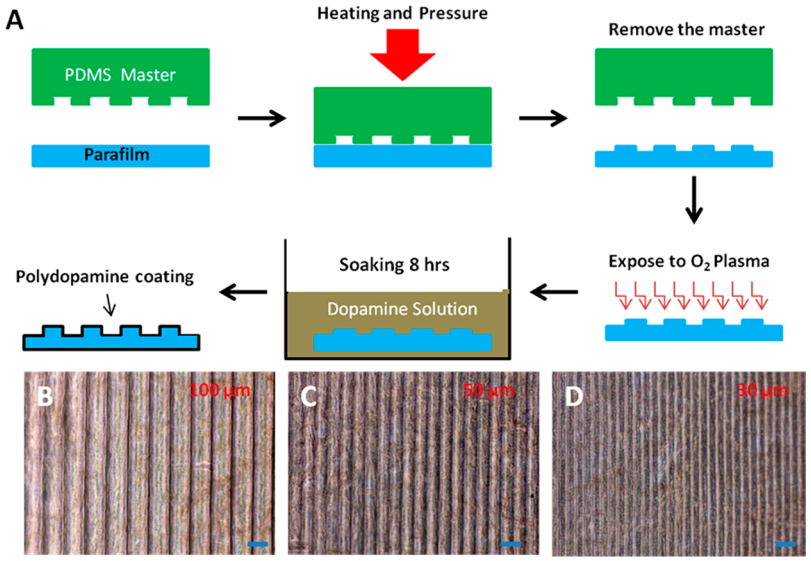

Figure 4. Generation of the micropatterned PDA-coated parafilms with different groove spaces. (A) Schematic of the generation of the micropatterned PDA-coated parafilm. (B–D) Optical images of PDA-coated parafilms with arrays of grooves (from panels B–D, the groove spacings are 100, 50, and 30 μm) (scale bar: 100 μm).

forces were measured using a digital force gauge (DS2-20N, IMADA, Japan). The cell responses to the tensile strains and micropatterns were assessed by specialized gene expression. In addition, the cell responses to the tensile strains and micropatterns in osteogenic media (DMEM/F12 supplemented with 10% (v/v) FBS, β-glycerophosphate (10 mM), ascorbic acid (50 mM), dexamethasone (0.1 mM), and 1% penicillin/streptomycin) were assessed by the expression of osteogenic genes.

2.8. Gene Expression. The total RNAs of cells on the films was extracted and purified using TRIzol Plus RNA purification kit (Sigma-Aldrich, USA) according to the manufacturer's instructions. One-step qRT-PCR was run using MyiQ2 two colors RT-PCR detection system (Bio-Rad, USA). The qRT-PCR reaction mix consisted of SuperScript III RT/Plantinum Taq Mix (Invitrogen, USA), ROX (Invitrogen, USA), primers, RNA template, and DEPC-treated water (Invitrogen, USA). Primer sequences were designed by Greiner Bio-One, Japan (Table S1, Supporting Information).[49,50]

2.9. Statistical Analysis. Data were expressed as means ± standard deviations (six replicates were conducted). Student's *t*-tests and ANOVA followed by Tukey's multiple comparison tests were performed to analyze differences between two experimental groups and among more than two experimental groups, respectively.

3. RESULTS AND DISCUSSION

3.1. Generating PDA-Coated Parafilm. PDA was deposited on an oxygen-plasma-treated parafilm via self-polymerization by dopamine oxidation in a weak alkaline buffer solution (pH = 8.5). As shown in Figure 1A, after 8 h of incubation in the dopamine solution, the parafilm darkened compared to the native parafilm, which was milky white. X-ray photoelectron spectroscopy (XPS) and scanning electron microscopy (SEM) were used to verify the formation of PDA on the parafilm's surface (Figure 1B and Figure S1, Supporting Information). The XPS spectrum of PDA-coated parafilm exhibits two peaks at approximately 399 and 513 eV, corresponding to $N1_S$ and $O1_S$ of the PDA coating, respectively. To determine the hydrophobicity of the PDA-coated parafilm, we performed a static water contact angle test (Figure 1C,D). The water contact angle of the pristine parafilm is 109.6°. The PDA-coated parafilm exhibits a significantly lower water contact angle, indicating that abundant hydrophilic groups were created on the surface of parafilm. In addition, the surface energy of the PDA-coated parafilm is approximately 16-fold higher than that of pristine parafilm, which may significantly promote cell adhesion.

The biocompatibility of the PDA-coated parafilm was also evaluated by studying the cytotoxicity with live/dead staining and cell counting kit (Figure 2). ADMSCs were seeded for 5 days and 12 days on the PDA-coated parafilm, the oxygen-plasma-treated parafilm, and native parafilm, respectively. After which the cell number on the PDA-coated parafilm was significantly higher than that of the oxygen-plasma-treated parafilm. Also, only a few cells were observed on the pristine parafilm due to its extremely high hydrophobicity. These results were also confirmed by live/dead staining. A larger number of cells grew on the PDA-coated parafilm and generated a cell network whereas significantly less cell proliferation was observed on the pristine parafilm. We also showed that cell proliferation on PDA-coated parafilm was similar to that of commercial cell culture plates.

The most pivotal process for cell adhesion on biomaterials is the deposition of extracellular matrix (ECM), such as laminin, collagen, and fibronectin. The process of protein immobilization on the surface of biomaterials was mediated by ECM secreted by cells or derived from cell culture medium.[51] To analyze the adsorption of proteins on PDA-modified parafilm, we immersed the PDA-coated parafilm in solutions containing fluorescein isothiocyanate labeled-bovine serum albumin (FITC-BSA) and rhodamine-labeled fibronectin (Figure 3). After 5 h of incubation, the immobilization of the fluorescent proteins on the PDA-coated parafilm was visualized. We did not observe significant protein adsorption on the surface of the unmodified parafilm or oxygen-plasma-treated parafilm, whereas a significantly higher amount of protein was adsorbed on the PDA-coated parafilm. We also confirmed this observation by using a protein quantificational assay (Figure 3C). These results showed that the immobilization of BSA and fibronectin on the PDA-coated parafilms was around 3- and 2-fold higher than that of the oxygen-plasma-treated parafilms, and approximately 32- and 25-fold higher than that of the pristine parafilms, respectively. Together, these results and previously studies

confirmed that the PDA-coated parafilm promote cell adhesion due to its higher ability to induce protein adsorption.[52−54]

3.2. Micropatterning PDA-Coated Parafilms. The process for the generation of different micropatterns on the PDA-coated parafilm is shown in Figure 4A. A pristine parafilm was placed on a flat PMMA slide and micromolded against a micropatterned PDMS stamp under pressure (5 N) at an elevated temperature (60 °C). After the micropatterned parafilm was molded, it was released from the PDMS stamp. Finally, the surface of the microstructured parafilm was modified with PDA. In this study, the PDA modification was conducted after the micropatterning for two main reasons. First, high temperatures were required to generate the micropatterns, whereas ambient temperatures were preferred for PDA deposition. Second, the micromolding process enlarged the surface area of the parafilm, which could damage the PDA coatings.

Here, we generated grooved micropatterns on PDA-coated parafilms to produce topographic cues for cell regulation. As shown in Figure 4B−D, array of grooves on PDMS stamps were successfully transferred onto PDA-coated parafilms. The replicated micropatterns exhibited fine microscale resolution. We subsequently seeded cells on the micropatterned parafilms to investigate the cell behavior regulated by the micropatterns (Figures 5A and S2, Supporting Information). The ADMSCs were cultured on the micropatterns for 3 days. To visualize the cells clearly, we used DAPI (blue color) and rhodamine phalloidin (red color) to stain nuclei and F-actin of cells, respectively. On the groove-patterned zone, we measured the alignment angles of the cell nuclei to confirm the cell alignment. Cells aggregated in the grooves of the micropatterned PDA-coated parafilm and exhibited significantly aligned structures. In contrast, the cells cultured on the flat PDA-coated parafilm exhibited random alignments. More than 80% and 40% of cells grown on the micropatterns with groove widths of 30 and 50 μm, respectively, were aligned with the same direction of groove, whereas only around 12% of cells were aligned on the flat PDA-coated parafilm (Figure 5B). The cell alignments were also confirmed by the orientation of F-actin. The F-actin of cells on the micropatterned surface was directed along the grooves. We also investigated the osteogenic gene expression of the stem cells seeded on different micropatterns with grooves. After stem cells were seeded onto various micropatterns, we used osteogenic media instead of common media to induce cell differentiation. The cells on the micropatterns with narrow grooves (the widths of groove are 30 and 50 μm) significantly promoted the expression of osteocalcin (a key osteogenic gene, which regulates the mineralization of bone) after 14 days of culture, indicating a higher osteogenic commitment of stem cells regulated by narrow grooves (Figure 5C). Due to the higher expression of osteocalcin (an important late osteogenic marker) of cells on the micropattern with a 50 μm groove, we used this micropattern to evaluate cell behavior in the following experiments.

3.3. Cell Behavior Regulated by Spatial and Mechanical Cues. To induce the elongation of the cells cultured on the micropatterned PDA-coated parafilm, we designed a PDMS device, which is shown schematically in Figure 6A. A small PDMS chamber was placed in a cell culture dish, and rectangular holes were cut through the right and left walls of the PDMS chamber. A strip of micropatterned PDA-coated parafilm was inserted through the two holes, and forces were exerted at the ends of the parafilm strip to stretch the parafilm, thus placing strain on the ADMSCs cultured on the parafilm

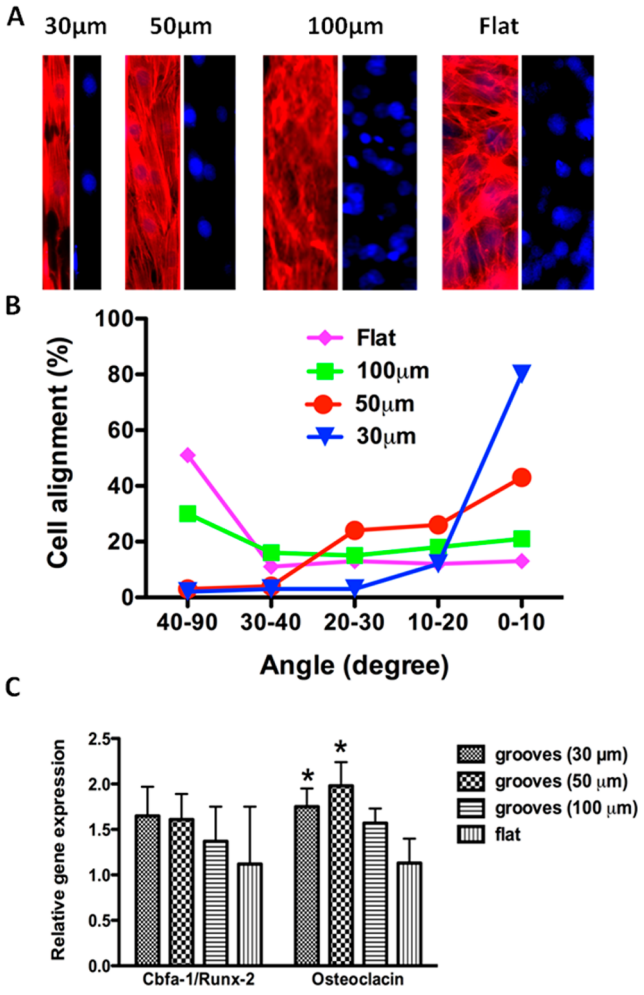

Figure 5. Cell alignments on the micropatterned PDA-coated parafilms with different groove spacings. (A) F-actin and nuclei staining of cells on the micropatterned PDA-coated parafilm with different groove spacings. (B) Aligned cell-nuclei counting of cells on the PDA-coated parafilm with grooved micropatterns and the flat PDA-coated parafilm after 3 days of culture. (C) Osteogenic gene expression of cells on the PDA-coated parafilms with different groove sizes after 14 days of culture. The * symbol indicates statistical significance when compared with cells on the flat PDA-coated parafilm at 95% confidence level. Expression levels were normalized with respect to the housekeeping gene β-actin.

(Figures S3 and S4, Supporting Information). Two different strains (2 and 2.5 N) were tested and compared with a cell culture on the PDA-coated parafilm in the absence of strain. The results indicated that cell elongation was determined by the strain because a higher strain induced a higher cell elongation. The cell elongation with the higher strain was approximately 1.3- and 1.8-fold higher than that driven by a lower strain or by nonstrain, respectively (Figure 6B,C). During the dynamic process of exerting stress on the parafilms, the cells with lower viability and activity detached from the parafilms because of their weaker adhesions. Therefore, the cell number on the stretched parafilm was slightly lower than that on the nonstrain parafilm (Figure 6D). In addition, we evaluated the cytoskeleton gene expression using quantitative reverse transcription-polymerase chain reaction (qRT-PCR) after 3 days and 5 days of culture (Figure 6E). The gene expression of SM22-α and α-actin of cells under higher strain was approximately 2.2- and 1.8-fold higher than that of the cells

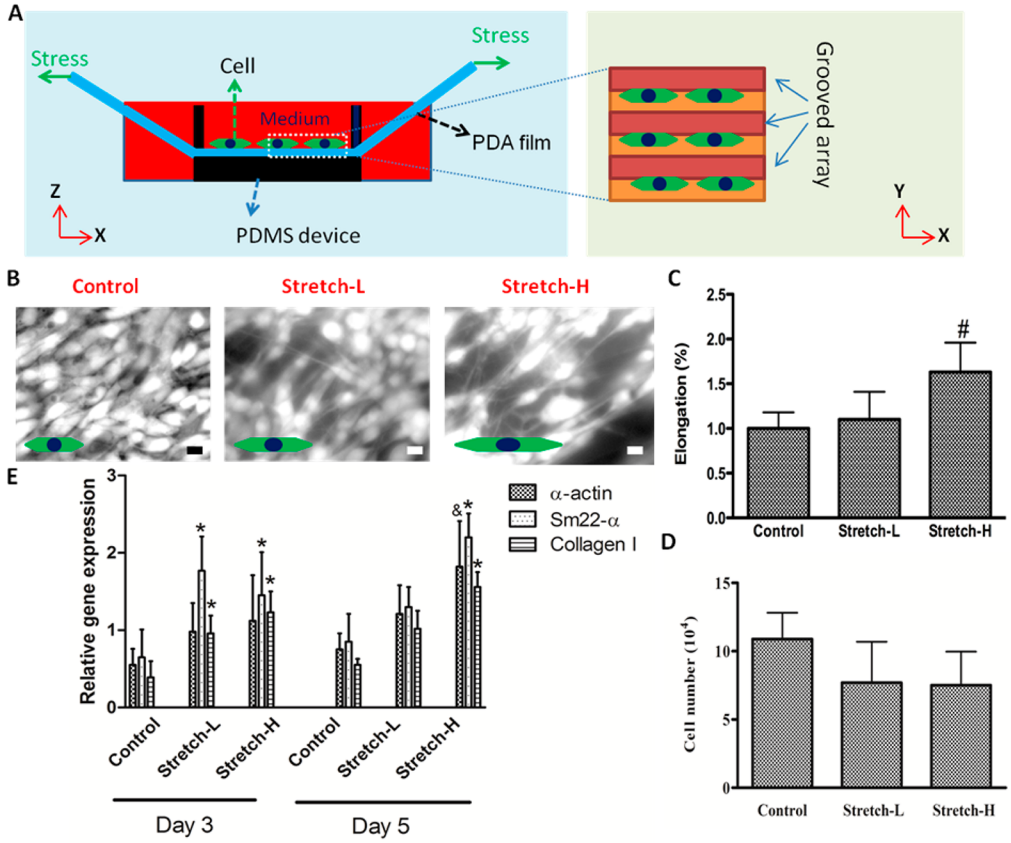

Figure 6. Morphology of stem cells treated by the platform constructed by the micropatterned PDA-modified parafilm (cells on the platform free of force were used as control, the exerted forces were paralleling to the direction of grooves). (A) Schematic of the device based on the micropatterned PDA-modified parafilms that induce the elongation of cells in an osteogenic microenvironment when stretched. (B) Cell elongation induced by the forces exerted on the parafilm in the devices (scale bar: 20 μm). (C) Cell elongation induced by the different forces (the $^{\#}$ symbol indicates statistical significance when compared with cells driven by a low force and control at 99% confidence level). (D) Viability of cells cultured on the micropatterned PDA-modified parafilms after being stretched. (E) Relative expression of cell-skeleton-related gene of cells under different forces induced by stretchable parafilms in the devices in a common culture medium after 3 and 5 days of culture (the $^{\&}$ and * symbols indicate statistical significance when compared with cells driven by a low force at 95% and 99% confidence levels, respectively; expression levels were normalized with respect to the housekeeping gene β-actin).

on the nonstretched film, respectively. The gene expression of SM22-α and α-actin of the cells with a lower strain was approximately 1.2- and 1.4-fold higher than that of the cells on the nonstretched parafilm, respectively. Furthermore, the expression of type I collagen of the cells with a higher strain was significantly stronger than that of the cells on the nonstretched parafilm. These results indicated that mechanical strains on the cells facilitate the expression of cytoskeleton-related genes, such as α-actin, and extracellular matrix-type I collagen.

We used the micropatterned PDA-coated parafilm to simulate the environment of the stem cells on the inner layer of the periosteum to induce osteogenesis of stem cells. Similarly, different strains were exerted on the stem cell-laden strip of micropatterned PDA-coated parafilm. The PDA-coated film with double elongation induced by the higher strain is similar to that of the original periosteum. As shown in Figure 7, the periosteum on the humerus (31 mm) is 2 times longer than the periosteum removed from the humerus (15 mm). Here, an osteogenic medium was used instead of the common cell culture medium used in the referenced study (DMEM+10% FBS) to stimulate the osteogenic commitment of the stem cells. After 12 days of culture, the expression of osteogenic protein and genes was evaluated on the PDA–parafilm-based platform (Figures 8 and S5, Supporting Information). The activity of

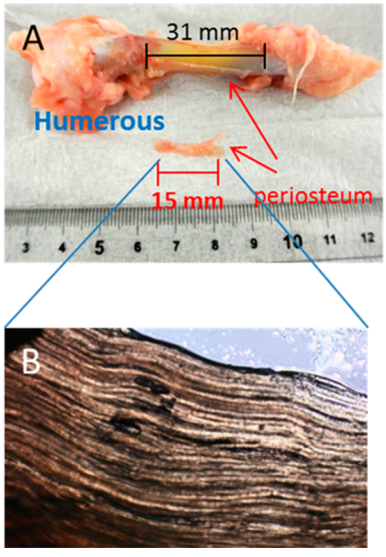

Figure 7. Morphology and stretchability of the periosteum. (A) Schematic of the periosteum on the bone and an optical image of the periosteum microstructure. (B) Schematic and image of the periosteum in the humerus (length: 31 mm) and the periosteum after being removed from the humerus (length: 15 mm).

dx.doi.org/10.1021/am5029236 | ACS Appl. Mater. Interfaces 2014, 6, 11915–11923

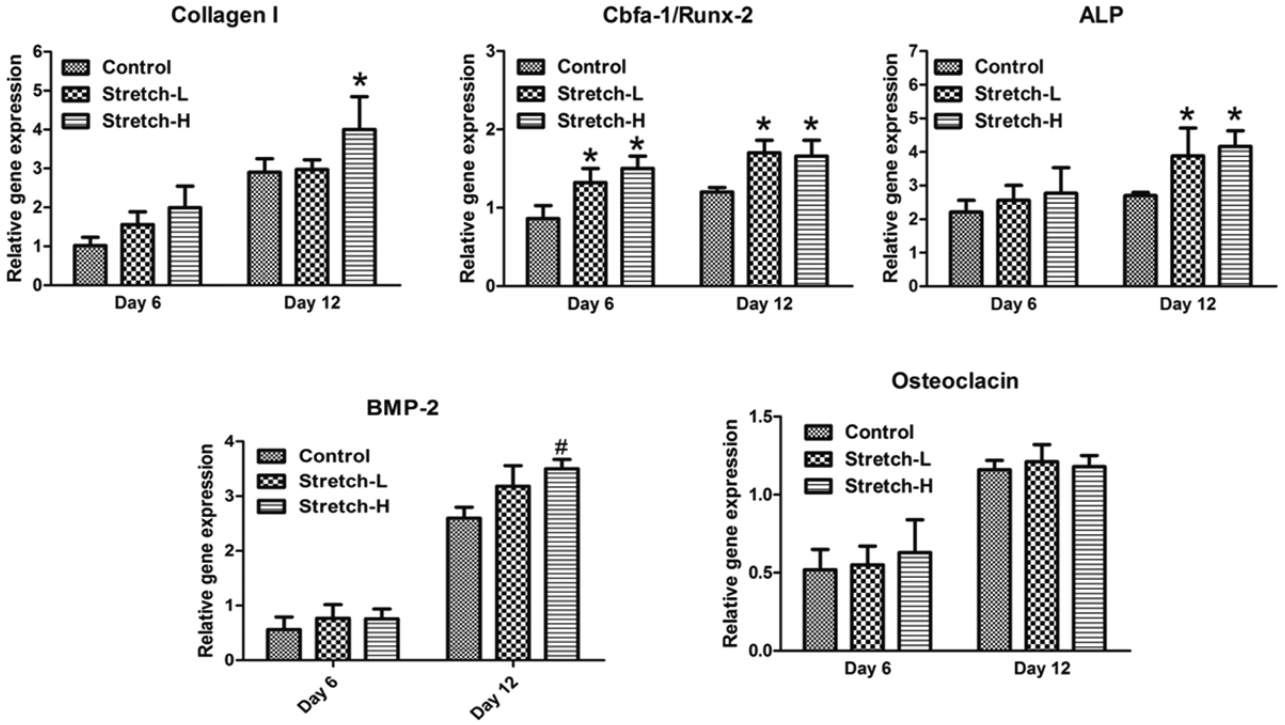

Figure 8. Expressions of osteogenic genes of cells in the osteogenic medium exposed to different forces induced by the stretchable parafilm in the devices after 6 and 12 days of culture (the # and * symbols indicate statistical significance when compared with control at 95% and 99% confidence levels, respectively). Expression levels were normalized with respect to the housekeeping gene β-actin.

alkaline phosphatase (ALP), gene expression of ALP (an early osteogenic marker), and Cbfa-1/Runx-2 (a key transcription factor related with osteoblast differentiation) of the cells driven by a higher strain were approximately 1.4-, 1.5-, and 1.4-fold higher than that of the cells on the nonstretched film, respectively. No remarkable difference was observed between the cells under the higher and lower strain conditions. However, the gene expression of type I collagen (main organic composition of bone) of the cells under the higher strain was approximately 1.3-fold higher than that of cells on the nonstretched parafilm and that of cells under the lower strain. Additionally, the cells driven by the higher strain showed stronger expression of BMP-2 (an osteoinductive growth factor) than the cells on the nonstretched parafilm.

The process of recognizing and responding to the mechanics of the surrounding matrix is critical for cell growth and function. In response to mechanical and spatial stimuli, the cells will use feedback to transfer these signals to biochemical signals and elicit cascade responses from mechanotransducer molecule activation, specialized gene expression, differentiation, and matrix remodeling.[55−57] Previous studies have indicated that microgrooved patterns promote osteogenesis in vitro and in vivo, because the osteogenesis was induced by orientating osteoblastic-like cells in bone and periosteum.[58−62] In this study, by simulating the mechanical and spatial conditions of the periosteum using micropatterned PDA-coated parafilm, we confirmed that the higher strain and spatial alignment of cells are of great importance for osteogenesis. Therefore, this platform provides a new method for understanding the effect of mechanical and spatial cues on cell differentiation.

4. CONCLUSION

In summary, a facile and efficient platform for cell culture and differentiation in an integrated environment that includes mechanical, chemical, biological, and topographic cues was developed. This platform uses a PDA-coated micropatterned parafilm. The micropatterned parafilm can effectively regulate spatial arrangement of cells. Specifically, the ADMSCs cultured on the platform exhibited significantly higher osteogenic commitment in response to mechanical and spatial cues induced by the modified parafilms compared to the one without stretch. Our finding may open a new door for stem cell differentiation studies using this modified parafilm platform.

■ ASSOCIATED CONTENT

Supporting Information

Real-time qRT-PCR primer sets, SEM images of PDA-coated parafilm before and after stretching, fluorescent images of F-actin and nuclei of cells cultured on the PDA-coated parafilm with grooves, dimensions of the devices based on PDA-coated parafilm for inducing cell elongations, optical images of PDA-coated parafilm before and after stretch, and alkaline phosphatase expression of cells cultured on the PDA-coated parafilms with different exerted forces. This material is available free of charge via the Internet at http://pubs.acs.org.

■ AUTHOR INFORMATION

Corresponding Authors

*X. Shi. E-mail: mrshixuetao@gmail.com.
*H. Wu. E-mail: chhkwu@ust.hk.

Notes

The authors declare no competing financial interest.

■ ACKNOWLEDGMENTS

X. Shi and L. Li contributed equally for this work. WPI Initiative funding from the Japan Society for the Promotion of Science and the Ministry of Education, Culture, Sports, Science,

and Technology (Japan) supports this work. H. Wu acknowledges the support of the Hong Kong RGC (GRF 604509 and GRF 605210).

REFERENCES

(1) Passier, R.; van Laake, L. W.; Mummery, C. L. Stem-Cell-Based Therapy and Lessons from the Heart. *Nature* **2008**, *453*, 322−329.
(2) Bianco, P.; Robey, P. G. Stem Cells in Tissue Engineering. *Nature* **2001**, *414*, 118−121.
(3) Rosenzweig, A. Cardic Cell Therapy-Mixed Results from Mixed Cells. *N. Engl. J. Med.* **2006**, *355*, 1274−1277.
(4) Brinster, R. L. Germline Stem Cell Transplantation and Transgenesis. *Science* **2002**, *296*, 2174−2176.
(5) Brunet, J. L.; McMahon, J. A.; McMahon, A. P.; Harland, R. M. Noggin, Cartilage Morphogenesis, and Joint Formation in the Mammalian Skeleton. *Science* **1998**, *280*, 1455−1457.
(6) Kirouac, D. C.; Zandstra, P. W. The Systematic Production of Cells for Cell Therapies. *Cell Stem Cell* **2008**, *3*, 369−381.
(7) Boheler, K. R.; Czyz, J.; Tweedie, D.; Yang, H.-T.; Anisimov, S. V.; Wobus, A. M. Differentiation of Pluripotent Embryonic Stem Cells into Cardiomyocytes. *Circ. Res.* **2002**, *91*, 189−201.
(8) Weiner, S.; Wagner, H. D. The Material Bone: Structure Mechanical Function Relations. *Annu. Rev. Mater. Sci.* **1998**, *28*, 271−298.
(9) Ochareon, P.; Herring, S. W. Growing the Mandible: Role of the Periosteum and Its Cells. *Anat. Rec.* **2007**, *290*, 1366−1376.
(10) Aaron, J. E.; Skerry, T. M. Intramembranous Trabecular Generation in Normal Bone. *Bone Miner.* **1994**, *25*, 211−230.
(11) Parfitt, A. M. Parathyroid Hormone and Periosteal Bone Expansion. *J. Bone Miner. Res.* **2002**, *17*, 1741−1743.
(12) Turner, R. T.; Riggs, B. L.; Spelsberg, T. C. Skeletal Effects of Estrogen. *Endocr. Rev.* **1994**, *15*, 275−300.
(13) Ushiku, C.; Adams, D. J.; Jiang, X.; Wang, L.; Rowe, D. W. Long Bone Fracture Repair in Mice Harboring GFP Reporters for Cells within the Osteoblastic Lineage. *J. Orthop. Res.* **2010**, *28*, 1338−1347.
(14) Einhorn, T. A. The Cell and Molecular Biology of Fracture Healing. *Clin. Orthop. Relat. Res.* **1998**, *355*, S7−S21.
(15) Shi, X.; Chen, S.; Zhao, Y.; Lai, C.; Wu, H. Enhanced Osteogenesis by a Biomimic Pseudo-Periosteum-Involved Tissue Engineering Strategy. *Adv. Healthcare Mater.* **2013**, *2*, 1229−1235.
(16) Shi, X.; Zhou, J.; Zhao, Y.; Li, L.; Wu, H. Gradient-Regulated Hydrogel for Interface Tissue Engineering: Steering Simultaneous Osteo/Chondrogenesis of Stem Cells on a Chip. *Adv. Healthcare Mater.* **2013**, *2*, 846−853.
(17) Guvendiren, M.; Burdick, J. A. Stem Cell Response to Spatially and Temporally Displayed and Reversible Surface Topography. *Adv. Healthcare Mater.* **2013**, *2*, 155−164.
(18) Discher, D. E.; Janmey, P.; Wang, Y. L. Tissue Cells Feel and Respond to the Stiffness of Their Substrate. *Science* **2005**, *310*, 1139−1143.
(19) Discher, D. E.; Mooney, D. J.; Zandstra, P. W. Growth Factors, Matrices, and Forces Combine and Control Stem Cells. *Science* **2009**, *324*, 1673−1677.
(20) Engler, A. J.; Sen, S.; Sweeney, H. L.; Discher, D. E. Matrix Elasticity Directs Stem Cell Lineage Specification. *Cell* **2006**, *126*, 677−689.
(21) Eyckmas, J.; Chen, C. S. Stem Cell Differentiation: Sticky Mechanical Memory. *Nat. Mater.* **2014**, *13*, 542−543.
(22) Chen, C. S. Mechanotransduction-a Filed Pulling Together? *J. Cell. Sci.* **2008**, *121*, 3285−3289.
(23) Augustin, G.; Antabak, A.; Davila, S. The Periosteum. Part 1: Anatomy, Histology and Molecular Biology. *Injury* **2007**, *38*, 1115−1130.
(24) Zamanian, B.; Masaeli, M.; Nichol, J. W.; Khabiry, M.; Hancock, M. J.; Bae, H.; Khademhosseini, A. Interface-Directed Self-Assembly of Cell-Laden Microgels. *Small* **2010**, *6*, 937−944.
(25) Proksch, S.; Steinberg, T.; Vach, K.; Hellwig, E.; Tomakidi, P. Shaping Oral Cell Plasticity to Osteogenic Differentiation by Human Mesenchymal Stem Cell Coculture. *Cell Tissue Res.* **2014**, *356*, 159−170.
(26) Zhang, J.-T.; Nie, J.; Mühlstädt, M.; Gallagher, H.; Pullig, O.; Jandt, K. D. Stable Extracellular Matrix Protein Patterns Guide the Orientation of Osteoblast-Like Cells. *Adv. Funct. Mater.* **2011**, *21*, 4079−4087.
(27) Tang, L.; Lin, Z.; Li, Y.-M. Effects of Different Magnitudes of Mechanical Strain on Osteoblasts *In Vitro*. *Biochem. Biophys. Res. Commun.* **2006**, *344*, 122−128.
(28) Foolen, J.; van Donkelaar, C. C.; Nowlan, N.; Murphy, P.; Huiskes, R.; Ito, K. Collagen Orientation in Periosteum and Perichondrium is Aligned with Preferential Directions of Tissue Growth. *J. Orthop. Res.* **2008**, *26*, 1263−1268.
(29) Glucksmann, A. The Role of Mechanical Stresses in Bone Formation In Vitro. *J. Anat.* **1942**, *76*, 231−239.
(30) Shi, X.; Zhao, Y.; Zhou, J.; Chen, S.; Wu, H. One-Step Generation of Engineered Drug-Laden Poly(lactic-co-glycolic acid) Micropatterned with Teflon Chips for Potential Application in Tendon Restoration. *ACS Appl. Mater. Interfaces* **2013**, *5*, 10583−10590.
(31) Paz, A. C.; Javaherian, S.; McGuigan, A. P. Tools for Micropatterning Epithelial Cells into Microcolonies on Transwell Filter Substrates. *Lab Chip* **2011**, *11*, 3440−3448.
(32) Ren, K.; Dai, W.; Zhou, J.; Su, J.; Wu, H. Whole-Teflon Microfluidic Chips. *Proc. Natl. Acad. Sci. U.S.A.* **2011**, *108*, 8162−8166.
(33) Dai, W.; Zheng, Y.; Lou, K. Q.; Wu, H. A Prototypic Microfluidic Platform Generating Stepwise Concentration Gradients for Real-Time Study of Cell Apoptosis. *Biomicrofluidics* **2010**, *4*, 024101.
(34) Lee, H.; Dellatore, S. M.; Miller, W. M.; Messersmith, P. B. Mussel-Inspired Surface Chemistry for Multifunctional Coating. *Science* **2007**, *318*, 426−430.
(35) Ryu, J.; Ku, S. H.; Lee, H.; Park, C. B. Mussel-Inspired Polydopamine Coating as a Universal Route to Hydroxyapatite Crystallization. *Adv. Funct. Mater.* **2010**, *20*, 2132−2139.
(36) Lee, H.; Lee, B. P.; Messersmith, P. B. A Reversible Wet/Dry Adhesive by Mussels and Geckos. *Nature* **2007**, *448*, 338−341.
(37) Yang, Z.; Tu, Q.; Zhu, Y.; Lou, R.; Li, X.; Xie, Y.; Maitz, M.; Wang, J.; Huang, N. Mussel-Inspired Coating of Polydopamine Directs Endothelial and Smooth Muscle Cell Fate for Re-Endothelialization of Vascular Devices. *Adv. Healthcare Mater.* **2012**, *1*, 548−552.
(38) Yan, J.; Yang, L.; Lin, M.-F.; Ma, J.; Lu, X.; Lee, P. S. Polydopamine Spheres as Active Templates for Convenient Synthesis of Various Nanostructures. *Small* **2013**, *9*, 596−603.
(39) Zheng, W.; Zhang, W.; Jiang, X. Precise Control of Cell Adhesion by Combination of Surface Chemistry and Soft Lithography. *Adv. Healthcare Mater.* **2013**, *2*, 95−108.
(40) Kim, S.; Park, C. B. Bio-Inspired Synthesis of Minerals for Energy, Environment, and Medicinal Applications. *Adv. Funct. Mater.* **2013**, *23*, 10−25.
(41) Lee, H.; Rho, J.; Messersmith, P. B. Facile Conjugation of Biomolecules onto Surfaces via Mussel Adhesive Protein Inspired Coating. *Adv. Mater.* **2009**, *21*, 431−434.
(42) Lynge, M. E.; van der Westen, R.; Postma, A.; Städler, B. Polydopamine-a Nature-Inspired Polymer Coating for Biomedical Science. *Nanoscale* **2011**, *3*, 4916−4928.
(43) Kurpinski, K.; Chu, J.; Hashi, C.; Li, S. Anisotropic Mechanosensing by Mesenchymal Stem Cells. *Proc. Natl. Acad. Sci. U.S.A.* **2006**, *103*, 16095−16100.
(44) Kolind, K.; Leong, K. W.; Besenbacher, F.; Foss, M. Guidance of Stem Cell Fate on 2D Patterned Surfaces. *Biomaterials* **2012**, *33*, 6626−6633.
(45) Wang, C.; Bai, J.; Gong, Y.; Zhang, H.; Shen, J.; Wang, D. A. The Control of Anchorage-Dependent Cell Behavior within a Hydrogel/Microcarrier System in an Osteogenic Model. *Biotechnol. Prog.* **2008**, *24*, 1142−1145.

(46) Sengupta, D.; Gilbert, P. M.; Johnson, K. J.; Blau, H. M.; Heilshorn, S. C. Protein-Engineered Biomaterials to Generate Human Skeletal Muscle Mimics. *Adv. Healthcare Mater.* **2012**, *1*, 785−789.
(47) Kanda, K.; Matsuda, T. Behavior of Arterial Wall Cells Cultured in Periodically Stretched Substrates. *Cell Transplant.* **1993**, *2*, 475−484.
(48) Aubin, H.; Nichol, J. W.; Huston, C.; Bae, H.; Sieminski, A. L.; Cropek, D. M.; Akhyari, P.; Khademhosseini, A. Directed 3D Cell Alignment and Elongation in Microengineered Hydrogels. *Biomaterials* **2010**, *31*, 6941−6951.
(49) Shi, X. T.; Wang, Y. J.; Ren, L.; Gong, Y. H.; Wang, D. A. Enhanced Alendronate Release From a Novel PLGA/Hydroxyapatite Microspheric System for Bone Repairing Applications. *Pharm. Res.* **2009**, *26*, 422−430.
(50) Wang, Y.; Shi, X.; Ren, L.; Yao, Y. C.; Wang, D. A. In Vitro Osteogenesis of Synovium Mesenchymal Cells Induced by Controlled Release of Alendronate and Dexamethasone from a Sintered Microspherical Scaffold. *J. Biomater. Sci. Polym. Ed.* **2010**, *21*, 1227−1238.
(51) Shi, X. T.; Ostrovidov, S.; Shu, Y.; Liang, X.; Nakajima, K.; Wu, H.; Khademhosseini, A. Microfluidic Generation of Polydopamine Gradients on Hydrophobic Surfaces. *Langmuir* **2014**, *30*, 832−838.
(52) Chien, C.-Y.; Tsai, W.-B. Poly(doapmine)-Assisted Immobilization of Arg-Gly-Asp Peptides, Hydroxyapatite, and Bone Morphogenic Protein-2 on Titanium to Improve the Osteogenesis of Bone Marrow Stem Cells. *ACS Appl. Mater. Interfaces* **2013**, *5*, 6975−6983.
(53) Rivera, J. G.; Messersmith, P. B. Polydopamine-Assisted Immobilization of Trypsin onto Monolithic Structures for Protein Digestion. *J. Sep. Sci.* **2012**, *35*, 1514−1520.
(54) Fletcher, D. A.; Mullins, R. D. Cell Mechanics and the Cytoskeleton. *Nature* **2010**, *463*, 485−492.
(55) Wang, N.; Butler, J. P.; Ingber, D. E. Mechanotransduction Across the Cell Surface and Through the Cytoskeleton. *Science* **2003**, *260*, 1124−1127.
(56) Chen, N.; Shi, X.; Witte, R.; Nakayama, K. S.; Ohmura, K.; Wu, H.; Takeuchi, A.; Hahn, H.; Esashi, M.; Gleiter, H.; Inoue, A.; Louzguine, D. V. A Novel Ti-Based Nanoglass Composite with Submicron-Nanometer-Sized Hierarchical Structures to Modulate Osteoblast Behaviors. *J. Mater. Chem. B* **2013**, *1*, 2568−2574.
(57) Shi, X.; Chen, S.; Zhou, J.; Yu, H.; Li, L.; Wu, H. Directing Osteogenesis of Stem Cells with Drug-Laden, Polymer-Microsphere-Based Micropatterns Generated by Teflon Microfluidic Chips. *Adv. Funct. Mater.* **2012**, *22*, 3799−3807.
(58) Namgung, S.; Baik, K. Y.; Park, J.; Hong, S. Controlling the Growth and Differentiation of Human Mesenchymal Stem Cells by the Arrangement of Individual Carbon Nanotubes. *ACS Nano* **2011**, *5*, 7383−7390.
(59) Higuchi, A.; Ling, Q. D.; Chang, Y.; Hsu, S. T.; Umezawa, A. Physical Cues of Biomaterials Guide Stem Cell Differentiation Fate. *Chem. Rev.* **2013**, *113*, 3297−3328.
(60) Klebe, R. J.; Caldwell, H.; Milam, S. Cells Transmit Spatial Information by Orienting Collagen Fibers. *Matrix* **1989**, *9*, 451−458.
(61) Matsugaki, A.; Fujiwara, N.; Nakano, T. Continuous Cyclic Stretch Induces Osteoblast Alignment and Formation of Anisotropic Collagen Fiber Matrix. *Acta Biomater.* **2013**, *9*, 7227−7235.
(62) Shi, X.; Fujie, T.; Saito, A.; Takeoka, S.; Hou, Y.; Shu, Y.; Chen, M.; Wu, H.; Khademhosseini, A. Periosteum-Mimetic Structures Made from Freestanding Microgrooves Nanosheets. *Adv. Mater.* **2014**, *26*, 3290−3296.